▌**Fluorescent Imaging** |*Hot Paper*|

Fluorescent Arylphosphonic Acids: Synergic Interactions between Bone and the Fluorescent Core

Yunus Zorlu,[a] Connor Brown,[b] Claudia Keil,[c] M. Menaf Ayhan,[a] Hajo Haase,[c] Richard B. Thompson,[d] Imre Lengyel,[b] and Gündoğ Yücesan*[c]

Abstract: Herein, we report the third generation of fluorescent probes (arylphosphonic acids) to target calcifications, particularly hydroxyapatite (HAP). In this study, we use highly conjugated porphyrin-based arylphosphonic acids and their diesters, namely 5,10,15,20-tetrakis[*m*-(diethoxyphosphoryl)phenyl]porphyrin (*m*-H$_8$TPPA-OEt$_8$) and 5,10,15,20-tetrakis [*m*-phenylphosphonic acid]porphyrin (*m*-H$_8$TPPA), in comparison with their positional isomers 5,10,15,20-tetrakis[*p*-(diisopropoxyphosphoryl)phenyl]porphyrin (*p*-H$_8$TPPA-*i*Pr$_8$) and 5,10,15,20-tetrakis [*p*-phenylphosphonic acid]porphyrin (*p*-H$_8$TPPA), which have phosphonic acid units bonded to sp^2 carbon atoms of the fluorescent core. The conjugation of the fluorescent core is thus extended to the (HAP) through sp^2-bonded $-$PO$_3$H$_2$ units, which generates increased fluorescence upon HAP binding. The resulting fluorescent probes are highly sensitive towards the HAP in rat bone sections. The designed probes are readily taken up by cells. Due to the lower reported toxicity of (*p*-H$_8$TPPA), these probes could find applications in monitoring bone resorption or adsorption, or imaging vascular or soft tissue calcifications for breast cancer diagnosis etc.

Dysregulation of calcium and phosphate homeostasis often leads to the pathological deposition of minerals, such as calcium carbonate (CC), calcium oxalate (CO), calcium phosphate (CP), calcium pyrophosphate (CPP), and hydroxyapatite (HAP) in many soft tissues,[1,2] such as those in the brain,[3] eye,[4] kidney[5] and skin.[2,6] The pathological deposition of these minerals causes these tissues to become inflexible or even brittle,

which can lead to uncontrolled access of extracellular materials or prevent the passive diffusion of molecules between cells and their environment, likely leading to cell death.[6] In addition, minerals like HAP can facilitate the retention of molecules by providing a binding surface for the pathological accumulation of molecules.[7a] Detecting and monitoring increased calcification can be a valuable early indication of breast cancer.[8] Conversely, monitoring the decrease in mineralization can be useful for assessing osteoporosis.[9] In addition, evidence is emerging that HAP deposition may play a role in the development and progression of age-related macular degeneration in the retina and neurodegeneration in the brain.[7] Therefore, monitoring calcification in health and disease is critical for diagnosis, monitoring progression and treatment.

There are several methods used to monitor calcification, some applicable in vivo while others only work in vitro.[10,11] A number of radiological techniques have the potential to detect calcification using radiography,[12,13] fluoroscopy,[13] conventional computed tomography (CT),[14] electron-beam tomography (EBT),[15,16] multi-detector CT,[17,18] intravascular ultrasound,[19,20] magnetic resonance imaging (MRI),[21] and transthoracic and transesophageal echocardiography.[22] However, most current methods cannot resolve smaller than millimeter sized mineralization and are usually invasive, costly and not well tolerated.[23] In vitro, the resolution can be significantly increased: The classic Von Kossa histochemical method relies on silver precipitation at sites of phosphate deposition,[24] while Alizarin Red S, a colorimetric label, is widely used to detect calcium deposition.[25] In combination these are effective, inexpensive and widely used methods to detect calcium phosphate mineralization in fixed cells in culture or postmortem tissue sections, but they are not very sensitive and subcellular resolution is limited.

[a] Dr. Y. Zorlu, Dr. M. M. Ayhan
Department of Chemistry, Faculty of Science
Gebze Technical University, 41400, Gebze-Kocaeli (Turkey)

[b] C. Brown, Dr. I. Lengyel
Wellcome-Wolfson Institute for Experimental Medicine
School of Medicine, Dentistry and Biomedical Science
Queen's University Belfast, Belfast BT9 7BL (UK)

[c] Dr. C. Keil, Prof. Dr. H. Haase, Dr. G. Yücesan
Technische Universität Berlin, Chair of Food Chemistry and Toxicology
Straße des 17. Juni 135, 10623 Berlin (Germany)
E-mail: yuecesan@tu-berlin.de

[d] Dr. R. B. Thompson
Department of Biochemistry and Molecular Biology
University of Maryland School of Medicine
Baltimore, Maryland 21201 (USA)

Chemistry–A European Journal

Communication
doi.org/10.1002/chem.202001613

Chemistry Europe
European Chemical
Societies Publishing

Fluorescent probes broadly offer better sensitivity than colori-metric ones, but existing stains such as Alizarin Red S, Xylenol Orange, or uranium have clear drawbacks such as modest se-lectivity among mineral phases, pH dependence, overlap of their fluorescence with tissue autofluorescence. Frangioni and Kovar's research groups developed the second generation fluorescent probes coupling HAP-binding moieties such as bis-phosphonate or tetracycline with red and near-infrared penta- or hepta-methine cyanine fluorescent moieties; the longer wavelength excitation and emission of these fluorophores sub-stantially reduces scattering and background fluorescence.[26–28] These probes were sensitive, selective, and usable in vivo in animal models, but are costly and by comparison with other probes that exhibit significant or unique changes in fluores-cence when binding to particular targets such as DNSA (dansylamide) with carbonic anhydrase,[29] the triphenyl meth-ane dye Auramine O with LADH (horse liver alcohol dehydro-genase) with,[30] or ethidium bromide with DNA,[31] their fluo-rescence is insensitive to whether they have bound to the (cal-cified) target or nonspecifically to something else. To address this latter issue, we sought to develop the third generation of fluorescent probes of calcification bearing phosphonic acid metal binding units which are bonded to one of the sp^2 carbon atoms of the fluorescent cores, with the goal of differ-entially perturbing the fluorescence of the probe when bound to calcified substrates, and thereby providing additional infor-mation. The use of such fluorophores would be important with respect to generating synergic interactions between the fluo-rescent core and the d orbitals of the target divalent metal ions.

In this sense, the phosphonic acid metal binding group has recently attracted significant attention in diverse scientific fields ranging from material science to medicine.[32,33] Our initial toxicity studies with aromatic phosphonic acids and phospho-nate metal-organic solids were promising for their in vivo ap-plications inasmuch as **p-H$_8$TPPA** exhibited no toxicity for an intestinal cell line at high concentrations.[34,35] One of the unex-plored properties of phosphonic acid metal binding groups is their potential role in imaging metal deposits in living systems. Our and Demadis' recent work, and Martell's early work from the 1970s all indicate that phosphonates exhibit high affinity towards alkali and alkaline earth metal ions, as well as divalent transition-metal ions.[35–39] In addition, the pKa_2 of phenylphos-phonic acid (PhPO$_3$H$_2$) is 7.44, giving PhPO$_3^{2-}$ a -2 charge under physiological pH.[40] Therefore, the use of phosphonic acid metal-binding unit(s) to target biologically significant diva-lent metal ions offers highly sensitive and pH-independent metal probes working near physiological pH. Bisphosphonates have been previously attached to cyanine (Osteosense®) and fluorescein moieties with long aliphatic hydrocarbon side chains to label target calcification with green or near infrared fluorescence.[39,41] The presence of sp^3 bonds in the aliphatic linker chain in these examples between the phosphonic acid and the fluorescent core in these examples merely used bis-phosphonates as recognition moieties and minimized any elec-tronic interactions between the fluorescent core and the phos-phonic acid metal binding unit. Therefore, such fluorescent

labels provide little if any change in fluorescence intensity upon HAP binding.[39,41–43] By comparison, the direct conjuga-tion of phosphonic acid metal binding group with an sp^2 carbon atom of the fluorescent core extends the conjugation of the fluorescent core up to the coordinated metal ion. Thus, it offers the prospect of the metal-ion binding the phospho-nate and affecting the fluorescence in useful ways. For in-stance, such binding and recognition of a metal ion might cause useful changes in fluorescence that might help discrimi-nate metal-bound fluorophores from unbound or non-specifi-cally bound fluorophores. Such fluorescent phosphonates con-taining direct sp^2 conjugation with the fluorescent core have not been reported in the literature, perhaps due to synthetic difficulties and the high energy requirement to form P–C bonds. Our recent research efforts with arylphosphonic acid synthesis have generated novel strategies to introduce phos-phonic acid around aromatic scaffolds, by Suzuki cross cou-pling or the d-catalyzed Arbuzov reaction.[44–47]

For this study, as seen in Scheme 1, we have synthesized 4 fluorescent probes. Two of them incorporate phenylphosphon-ic acid as the HAP binding unit with highly conjugated porphy-rin cores, namely 5,10,15,20-tetrakis[p-phenylphosphonic acid]-porphyrin (**p-H$_8$TPPA**) and 5,10,15,20-tetrakis[m-phenylphos-phonic acid]porphyrin (**m-H$_8$TPPA**) (Figure 1; please see the Supporting Information for synthesis details). **p-H$_8$TPPA** has four *para*-positioned PPA units promoting direct conjugation between the HAP and the fluorescent core. On the other hand, **m-H$_8$TPPA** has four *meta*-positioned PPA units creating a more protective environment between the fluorescent porphyrin core and the HAP. We then explored their potential for binding hydroxyapatite. As a control group we used the isopropyldiest-er and ethyldiester analogues of **p-H$_8$TPPA** and **m-H$_8$TPPA**, namely **p-H$_8$TPPA-iPr$_8$** and **m-H$_8$TPPA-OEt$_8$** (see the Supporting
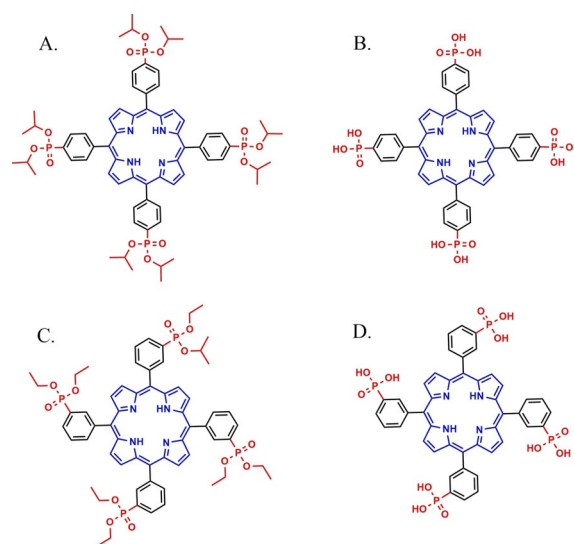
Scheme 1. The fluorescent probes used in this study: A) 5,10,15,20-Tetra-kis[p-(diisopropoxyphosphoryl)phenyl]porphyrin (**p-H$_8$TPPA-iPr$_8$**).
B) 5,10,15,20-Tetrakis [p-phenylphosphonic acid]porphyrin (**p-H$_8$TPPA**).
C) 5,10,15,20-Tetrakis[m-(diethoxyphosphoryl)phenyl]porphyrin (**m-H$_8$TPPA-OEt$_8$**). D) 5,10,15,20-Tetrakis [m-phenylphosphonic acid]porphyrin (**m-H$_8$TPPA**).

Chemistry–A European Journal

Communication
doi.org/10.1002/chem.202001613

Chemistry Europe
European Chemical
Societies Publishing
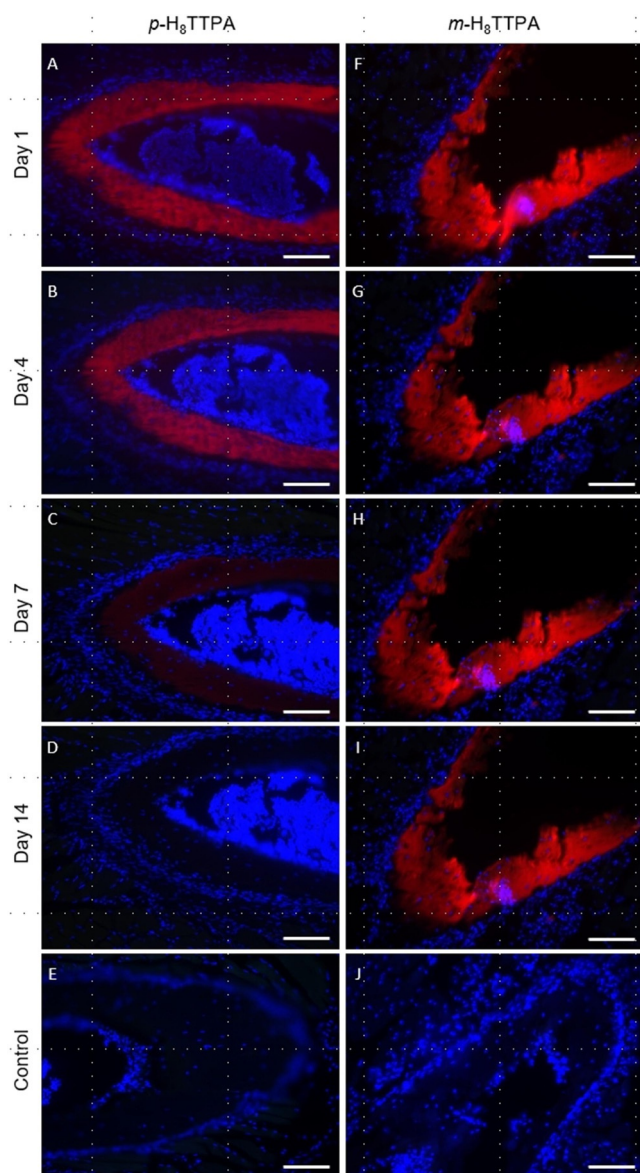
Figure 1. Mouse ribs incubated with either *p*-H$_8$TPPA ($\lambda_{ex/em}$ 595/613 nm; exposure time −200 ms) or *m*-H$_8$TPPA ($\lambda_{ex/em}$ 578/603 nm; exposure time −100 ms) diluted to 1 mg mL^{-1} in HEPES (A–E or F–J, respectively) and counter-stained with DAPI ($\lambda_{ex/em}$ 359/461 nm; exposure time: −200 or 100 ms, respectively). Images were captured on the day of staining (A and F), as well as after 4 days (B and G), 7 days (C and H), and 14 days (D and I). A negative control of mouse ribs incubated with each buffer alone is also included (E and J, respectively). Scale bar = 100 μm.

Information for detailed synthesis). A previous synthesis of *p*-H$_8$TPPA relied on the Ni-catalyzed Arbuzov reaction.[48] Therefore, *p*-H$_8$TPPA that is synthesized using this route usually has Ni bound to the nitrogens in the porphyrin core. In this study, we have used an alternative method using Pd-catalyzed Arbuzov reaction to obtain metal free *p*-H$_8$TPPA. (please see the Supporting Information for synthesis details, NMR, FTIR spectra, and the crystallographic tables).

To probe their HAP binding properties in a biological matrix, we have used cross sectioned mouse ribs as an example for naturally occurring HAP. The sections were incubated with *p*-

H$_8$TPPA, *m*-H$_8$TPPA and *p*-H$_8$TPPA-*i*Pr$_8$ at concentrations ranging from 0.01 to 1.0 mg mL^{-1} in HEPES buffer for varying times at room temperature, then imaged by fluorescence microscopy (details below in the figure legends), to assess HAP binding capability. Ribs incubated with 1 mg mL^{-1} *p*-H$_8$TPPA showed a greater fluorescence intensity than both 0.1 mg mL^{-1} and 0.01 mg mL^{-1} (Figure S17 A–C, respectively), whilst still showing clear fluorescence signal at the lowest concentration of 0.1 mg mL^{-1} used here.

This indicates that the dye binding to HAP is concentration dependent. When the mouse ribs were incubated with 1 mg mL^{-1} *p*-H$_8$TPPA in HEPES for differing times from 120 to 10 mins (Figure S18 A–E), there was a clear decrease in fluorescence intensity but even the 10 min short incubation yielded an appreciable fluorescence compared to the negative control (Figure S18 E compared to Figure S18 F). When ribs were incubated with *p*-H$_8$TPPA diluted to 1 mg mL^{-1} in different buffers, there was no clear difference between the fluorescence intensity of HEPES, PBS, TBS (Figure S19 A–C, respectively). However, when *p*-H$_8$TPPA was diluted in dH$_2$O (Figure S19 D), there was no fluorescent signal observed. Sections were re-imaged at several time points after the original microscopy sessions to observe the stability of labeling. There was a noticeable decrease in fluorescence intensity in all of the solvents although signal diminished faster in HEPES buffer than in PBS or TBS (Figure S20). At the two week time point there was still a weak fluorescent signal observed for *p*-H$_8$TPPA diluted in PBS, but not for the other buffers (Figure S20 N compared to Figure S20 M, O and P). No signal was associated with incubating the ribs with the solvents as a negative control (Figure S20 Q-T)

The phosphonic acid moieties in *m*-H$_8$TPPA are more protected compared to the *para*-positioned *p*-H$_8$TPPA. When mouse ribs were incubated with different concentrations of *m*-H$_8$TPPA, (1 to 0.01 mg mL^{-1} in HEPES buffer) we found little to no difference in the fluorescence intensities (Figure S21 A–C, respectively). When the mouse ribs were incubated with 1 mg mL^{-1} *m*-H$_8$TPPA in HEPES for differing times, 10 to 120 mins, there were no appreciable difference in the fluorescence intensities at the different incubation times (Figure S22 A–E, respectively) while the fluorescent intensities were clearly distinguishable from HEPES alone (Figure S22 F). Imaging of the sections were repeated two weeks following the original microscopy and we found no noticeable decrease in fluorescence intensity between ribs incubated with 1 mg mL^{-1} *m*-H$_8$TPPA in HEPES buffer and imaged on the day of staining compared with images taken 4, 7 and 14 days later (Figure 1 F–I, respectively). This is a noticeable difference compared to *p*-H$_8$TTPA, with a less protected structure, where there is a loss of fluorescent signal with increasing time after initial staining (Figure 1 A–D, respectively). This could be associated with the more protected HAP phosphonic acid interaction in the *meta* position limiting the interactions with the surrounding molecules buffers etc. Again, no signal was associated with incubating the ribs with HEPES only as a negative control (Figure 1 E and I, respectively).

As seen in Figure 2, the absorbance peak (Figure 2 A) of *p*-H$_8$TTPA in PBS, TBS and HEPES with the addition of HAP corre-

Chemistry–A European Journal

Communication
doi.org/10.1002/chem.202001613

Chemistry Europe
European Chemical
Societies Publishing
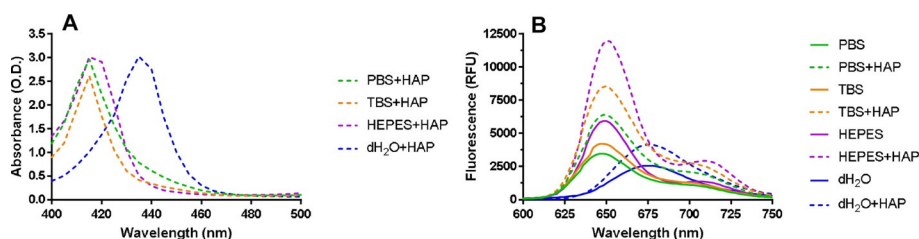
Figure 2. The absorbance (A) and fluorescence (B) spectra of 0.01 mg mL^{-1} **p-H$_8$TPPA** in the presence (dashed lines) and absence (solid lines) of HAP. The dye was diluted to 0.01 mg mL^{-1} in PBS (pH 7.4, green), TBS (pH 7.4, orange), HEPES (pH 7.4, purple) and dH$_2$O with absorbance and fluorescence spectra obtained using the Flexstation 3 microplate reader.

sponds with the absorbance of the dye in *d*-DMSO (Figure S16). There is a noticeable shift in the absorbance peak maximum when diluted in dH$_2$O, from 415 nm to 435 nm, which suggests a shift in the fluorescent properties of the dye due to protonation. This is also reflected in the maximal peak of the fluorescence intensity (Figure 2B), with a shift from λ_{em} 646–648 nm for PBS, TBS and HEPES to λ_{em} 675 nm when diluted in dH$_2$O. The fluorescence intensity of **p-H$_8$TPPA** is also substantially increased by 1.8-, 2.0-, 2.0-, and 1.6-fold upon HAP binding of the fluorescent probe **p-H$_8$TPPA** in PBS, TBS, HEPES and dH$_2$O, respectively (Figure 2B, solid vs. dashed lines). Previously reported bisphosphonate fluorophores had sp^3 aliphatic carbons between the fluorescent core and HAP binding, therefore, such systems merely functioned as fluorescent labels with no change in emission due to HAP binding since they lacked synergistic interaction between the HAP and the fluorescent core. Phosphonic acids that have direct sp^2 bonds to the fluorescent core could extend the conjugation of the fluorescent core to the HAP and thereby could initiate changes in the ground and excited states resulting in quenching or enhancing the fluorescence emission. As seen in Figure 2(B), upon binding of HAP, **p-H$_8$TPPA** produces increased fluorescence supporting this hypothesis; **p-H$_8$TPPA** is thus the first example of a single sp^2 bonded phosphonic acid unit targeting HAP in the literature.

Comparable experiments with mouse rib sections were conducted using the isopropyldiester forms **p-H$_8$TPPA-*i*Pr$_8$** and **m-H$_8$TPPA-OEt$_8$** (See Scheme 1a and 1c) as stains. We found a complete lack of HAP-associated staining with these compounds suggesting that the interaction of phosphonates with HAP was reduced by the isopropylester groups on the phosphonates, preventing binding and interaction of the fluorescent porphyrin core with the HAP. We also noted that the presence of hydrophobic isopropyl groups dramatically reduced their solubilities in the aqueous.

Aiming to use phenylphosphonic acid functionalized porphyrins in in vivo applications, the negative charge on the deprotonated phosphonate might be a handicap by limiting cell permeability. Optional demasking of phosphonate esters in metabolic surroundings might occur, recreating the metal binding PhPO$_3^{2-}$. This possibility led us to examine **p-H$_8$TPPA** and **p-H$_8$TPPA-*i*Pr$_8$** suitability for in vivo cellular experiments by testing their permeability on proliferating human THP-1 monocytes. The cells were probed with either **p-H$_8$TPPA** or **p-H$_8$TPPA-*i*Pr$_8$** in a HEPES-based buffer containing 0.3% bovine

serum albumin. Albumin binds a wide variety of hydrophobic ligands under physiological conditions, so we assumed an improved solubility/accessibility for the isopropyl diester molecule for cellular uptake. In addition, albumin is a regular component of culture media.

As seen in Figure 3, the fluorescence spectra of **p-H$_8$TPPA**-loaded THP-1 cells very much resembles the characteristics of the sensor diluted in HEPES-buffer (see Figure 1 A,F). Thus, beyond the low toxicity **p-H$_8$TPPA** provides two more positives -cell permeability and cellular retention- desirable for imaging applications. **p-H$_8$TPPA-*i*Pr$_8$** was much less efficient in labeling the THP-1 cells (see Figure S23). We hypothesize that the phenylphosphonic acid porphyrins, being somewhat amphipathic, were able to penetrate the cell membrane, whereas the more nonpolar esters were not as efficient.

In conclusion, herein, we have reported next-generation fluorescent probes to target calcifications, namely **p-H$_8$TPPA**, **m-H$_8$TPPA**, **p-H$_8$TPPA-*i*Pr$_8$**, and **m-H$_8$TPPA-OEt$_8$**, in which the phosphonic acid metal binding unit(s) are exclusively bonded to sp^2 carbon atoms of the fluorescent core. sp^2 bonding of the metal binding unit to the fluorescent core further extended the conjugation of the fluorescent core to the HAP, leading to significant increase in fluorescence upon HAP binding. We further used these fluorescent probes to target the HAP in mouse ribs and observed their interaction with human cells. Both **m-H$_8$TPPA** and **m-H$_8$TPPA** have shown HAP specific binding in rat bone sections. The more protected metal binding nature of the **m-H$_8$TPPA** resulted in longer fluorescence period compared to its positional isomer **p-H$_8$TPPA**. As a control, we have also synthesized phosphonatediesters of the synthesized fluorescent probes, which showed no HAP binding. **p-H$_8$TPPA** can travel through the cellular membrane, whereas the pres-
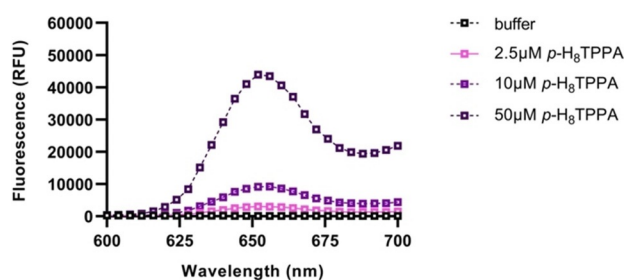
Figure 3. Fluorescence spectra of THP-1 monocytes cells incubated with **p-H$_8$TPPA**.

Chemistry–A European Journal

Communication
doi.org/10.1002/chem.202001613

Chemistry Europe
European Chemical
Societies Publishing

ence of bulky and hydrophobic isopropyl groups in **p-H$_8$TPPA-iPr$_8$** hindered their passage through the cellular membrane. This is the first study utilizing sp^2-bonded phosphonic acids with the fluorescent cores to target HAP mineralizations. We have shown that compact fluorescent probes with phosphonic acid metal binding group(s) may be used to monitor microcalcifications and calcifications. In addition, their easy acceptance into the cellular matrix indicate that they could be used to target organelle-specific calcifications such as mitochondrial calcifications. The reported low toxicity of **p-H$_8$TPPA** and the new synthetic methods indicate that they can be used in targeting wide range of calcifications in vivo. We are currently developing our library to target organelle specific calcifications.

Animal Experiments

Animal procedures were approved by Queen's University Belfast Animal Welfare and Ethical Review Body (AWERB) and authorized under the UK Animals (Scientific Procedures) Act 1986. Animal use conformed to the standards of the ARVO Statement for the Use of Animals in Ophthalmic and Vision Research and with European Directive 210/63/EU.

Acknowledgements

Conflict of interest

G.Y. and H.H. have pending patent protecting some of the presented data.

[1] A. Vallejo-Illarramendi, I. Toral-Ojeda, G. Aldanondo, A. López de Munain, *Expert. Rev. Mol. Med.* **2014**, *16*, E16.

[2] "Soft Tissue Calcification and Ossification": A. H. Newberg in *Imaging of Arthritis and Metabolic Bone Disease* (Ed.: B. N. Weissman), Elsevier, **2009**, chap. 39, pp. 681–696.

[3] E. M. Ramos, J. Oliveira, M. J. Sobrido, G. Cappola, *Primary Familial Brain Calcification* (Eds.: M. P. Adam, H. H. Ardinger, R. A. Pagon, S. E. Wallace, L. J. H. Bean, K. Stephens, A. Amemiya) **2004**, Apr 18 [Updated 2017 Aug 24]. GeneReviews® [Internet]. Seattle (WA): University of Washington, Seattle; 1993–2020.

[4] M. G. Pilgrim, I. Lengyel, A. Lanzirotti, M. Newville, S. Fearn, E. Emri, J. C. Knowles, J. D. Messinger, R. W. Read, C. Guidry, C. A. Curcio, *Invest. Ophthalmol. Vis. Sci.* **2017**, *58*, 708–719.

[5] S. M. Moe, N. X. Chen, *J. Am. Soc. Nephrol.* **2008**, *19*, 213–216.

[6] a) G. M. Garcia, G. C. McCord, R. Kumar, *Semin. Musculoskelet Radiol.* **2003**, *7*, 187–193; b) M. E. Witte, A. M. Schumacher, C. F. Mahler, J. P. Bewersdorf, J. Lehmitz, A. Scheiter, P. Sánchez, P. R. Williams, O. Griesbeck, R. Naumann, T. Misgeld, M. Kerschensteiner, *Neuron* **2019**, *101*, 615–624.

[7] a) R. B. Thompson, V. Reffatto, J. G. Bundy, E. Kortvely, J. M. Flinn, A. Lanzirotti, E. A. Jones, D. S. McPhail, S. Fearn, K. Boldt, M. Ueffing, S. G. Ratu, L. Pauleikhoff, A. C. Bird, I. Lengyel, *Proc. Natl. Acad. Sci. USA* **2015**, *112*, 1565–1570; b) A. C. S. Tan, M. G. Pilgrim, S. Fearn, S. Bertazzo, E. Tsolaki, A. P. Morrell, M. Li, J. D. Messinger, R. Doiz-Marco, J. Lei, M. G. Nittala, S. R. Sadda, I. Lengyel, K. B. Freund, C. A. Curcio, *Sci. Transl. Med.* **2018**, *10*, eaat4544; c) T. C. von Erlach, S. Bertazzo, M. A. Wozniak, C.-M. Horejs, S. A. Maynard, S. Attwood, B. K. Robinson, H. Autefage, C. Kallepitis, A. del Río Hernández, C. S. Chen, S. Goldoni, M. M. Stevens, *Nat. Mater.* **2018**, *17*, 237–242; d) V. Tadic, A. Westenberger, A. Domingo, D. Alvarez-Fischer, C. Klein, M. Kasten, *JAMA Neurol.* **2015**, *72*, 460–467.

[8] J. J. Mordang, A. Gubern-Mérida, A. Bria, F. Tortorella, R. M. Mann, M. J. M. Broeders, G. J. den Heeten, N. Karssemeijer, *Breast Cancer Res. Treat.* **2018**, *167*, 451–458.

[9] K. Ganesan, P. Bansal, A. Goyal, R. Douglas, *Bisphosphonate*, StatPearls Publishing, **2020**.

[10] A. Zaheer, M. Murshed, A. M. De Grand, T. G. Morgan, G. Karsenty, J. V. Frangioni, *Arterioscler. Thromb. Vasc. Biol.* **2006**, *26*, 1132–1136.

[11] J. S. Lee, J. D. Morrisett, C.-H. Tung, *Atherosclerosis* **2012**, *224*, 340–347.

[12] V. Freire, T. P. Moser, M. Lepage-Saucier, *Insights into Imaging* **2018**, *9*, 477–492.

[13] "Detection and Quantification of Coronary Calcification": R. Vliegenthart in *Coronary Radiology. Medical Radiology* (Eds.: M. Oudkerk), Springer, Berlin, Heidelberg, **2004**, pp. 175–184.

[14] C. R. Becker, A. Knez, T. F. Jakobs, S. Aydemir, A. Becker, U. J. Schoepf, R. Bruening, R. Haberl, M. F. Reiser, *Eur. Radiol.* **1999**, *9*, 620–624.

[15] R. Vliegenthart, B. Song, A. Hofman, J. C. M. Witteman, M. Oudkerk, *Radiology* **2003**, *229*, 520–525.

[16] J. P. Shields, Jr., C. H. Mielke, T. H. Rockwood, R. A. Short, F. K. Viren, *Am. J. Card. Imaging* **1995**, *9*, 62–66.

[17] L. Saba, G. Mallarin, *Am. J. Neuroradiol.* **2009**, *30*, 1445–1450.

[18] D. T. Boll, E. M. Merkle, E. K. Paulson, R. A. Mirza, T. R. Fleiter, *Radiology* **2008**, *249*, 119–126.

[19] G. S. Mintz, *JACC-Cardiovasc. Imaging.* **2015**, *8*, 461–471.

[20] N. B. Senguttuvan, S. Kumar, W.-S. Lee, S. Mishra, J. H. Cho, J. E. Kwon, S. H. Hyeon, Y. S. Jeong, H. Won, S. Y. Shin, K. J. Lee, T. H. Kim, C. J. Kim, S.-W. Kim, *Plos One* **2016**, *11*, e0165885.

[21] A. Fatemi-Ardekani, C. Boylan, M. D. Noseworthy, *Med. Phys.* **2009**, *36*, 5429–5436.

[22] S. Schwartzenberg, Y. Shapira, M. Vaturi, M. Nassar, A. Hamdan, I. Yedidya, H. Ofek, S. Kazum, D. Monakier, R. Kornowski, A. Sagie, *Eur. Heart J. Cardiovasc. Imaging* **2020**, *21*, jez319.805.

[23] Y. Wang, M. T. Osborne, B. Tung, M. Li, Y. Li, *J. Am. Heart Assoc.* **2018**, *7*, e008564.

[24] J. Rungby, M. Kassem, E. F. Eriksen, G. Danscher, *Histochem. J.* **1993**, *25*, 446–451.

[25] A. Bensimon-Brito, J. Cardeira, G. Dionísio, A. Huysseune, M. L. Cancela, P. E. Witten, *BMC Dev. Biol.* **2016**, *16*, 2.

[26] "Red and Near-Infrared Fluorometry": R. B. Thompson in *Topics in Fluorescence Spectroscopy Vol. 4: Probe Design and Chemical Sensing* (Eds.: J. R. Lakowicz), **1994**, New York, Plenum Press, pp. 151–181.

[27] G. Hong, A. Antaris, H. Dai, *Nat. Biomed. Eng.* **2017**, *1*, 0010.

[28] J. L. Kovar, X. Xu, D. Draney, A. Cupp, M. A. Simpson, D. M. Olive, *Anal. Biochem.* **2011**, *416*, 167–173.

[29] R. F. Chen, J. C. Kernohan, *J. Biol. Chem.* **1967**, *242*, 5813–5823.

[30] R. H. Conrad, J. R. Heitz, L. Brand, *Biochemistry* **1970**, *9*, 1540–1546.

[31] J.-B. LePecq, C. Paoletti, *J. Mol. Biol.* **1967**, *27*, 87–106.

[32] G. Yücesan, Y. Zorlu, M. Stricker, J. Beckmann, *Coord. Chem. Rev.* **2018**, *369*, 105–122.

[33] R. von Moos, L. Costa, E. Gonzalez-Suarez, E. Terpos, D. Niepel, J.-J. Body, *Cancer Treat. Rev.* **2019**, *76*, 57–67.

[34] A. Bulut, M. Maares, K. Atak, Y. Zorlu, B. Çoşut, J. Zubieta, J. Beckmann, H. Haase, G. Yücesan, *CrystEngComm* **2018**, *20*, 2152–2158.

[35] M. Maares, M. M. Ayhan, K. B. Yu, A. O. Yazaydin, K. Harmandar, H. Haase, J. Beckmann, Y. Zorlu, G. Yücesan, *Chem. Eur. J.* **2019**, *25*, 11214–11217.

[36] R. J. Motekaitis, I. Murase, A. E. Martell, *Inorg. Chem.* **1976**, *15*, 2303–2306.

[37] T. K. Hurst, D. Wang, R. B. Thompson, C. A. Fierke, *Biochim. Biophys. Acta Proteins Proteomics* **2010**, *1804*, 393–403.

[38] I. R. Salcedo, R. M. P. Colodrero, M. Bazaga-Garca, A. Vasileiou, M. Papadaki, P. Olivera-Pastor, A. Infantes-Molina, E. R. Losilla, G. Mezei, A. Cabeza, K. D. Demadis, *CrystEngComm* **2018**, *20*, 7648–7658.

[39] H. Hyun, H. Wada, K. Bao, J. Gravier, Y. Yadav, M. Laramie, M. Henary, J. V. Frangioni, H. S. Choi, *Angew. Chem. Int. Ed.* **2014**, *53*, 10668–10672; *Angew. Chem.* **2014**, *126*, 10844–10848.

[40] K. Nagarajan, K. P. Shelly, R. R. Perkins, R. Stewart, *Can. J. Chem.* **1987**, *65*, 1729–1733.

[41] A. M. Sim, N. A. Rashdan, L. Cui, A. J. Moss, F. Nudelman, M. R. Dweck, V. E. MacRae, A. N. Hulme, *Sci. Rep.* **2018**, *8*, 17360.

[42] K. R. Bhushan, E. Tanaka, J. V. Frangioni, *Angew. Chem. Int. Ed.* **2007**, *46*, 7969–7971; *Angew. Chem.* **2007**, *119*, 8115–8117.

[43] S. Sun, K. M. Błażewska, A. P. Kadina, B. A. Kashemirov, X. Duan, J. T. Triffitt, J. E. Dunford, R. Graham, G. Russell, F. H. Ebetino, A. J. Roelofs, F. P. Coxon, M. W. Lundy, C. E. McKenna, *Bioconjugate Chem.* **2016**, *27*, 329–340.

[44] A. Schütrumpf, A. Duthie, E. Lork, G. Yücesan, J. Beckmann, *Z. Anorg. Allg. Chem.* **2018**, *644*, 1134–1142.

[45] A. Schütrumpf, E. Kirpi, A. Bulut, F. L. Morel, M. Ranocchiari, E. Lork, Y. Zorlu, S. Grabowsky, G. Yücesan, J. Beckmann, *Cryst. Growth Des.* **2015**, *15*, 4925–4931.

[46] A. Bulut, Y. Zorlu, M. Wörle, S. Paşa, H. Kurt, J. Zubieta, J. Beckmann, G. Yücesan, *Eur. J. Inorg. Chem.* **2016**, 3506–3512.

[47] A. Bulut, Y. Zorlu, M. Wörle, A. Çetinkaya, H. Kurt, B. Tam, A. Özgür Yazaydin, J. Beckmann, G. Yücesan, *ChemistrySelect* **2017**, *2*, 7050–7053.

[48] T. Rhauderwiek, H. Zhao, P. Hirschle, M. Döblinger, B. Bueken, H. Reinsch, D. De Vos, S. Wuttke, U. Kolb, N. Stock, *Chem. Sci.* **2018**, *9*, 5467–5478.